Overview of the Microstructures of a Zirconium Alloy Cladding Tube after High-Temperature Steam Oxidation

Cheol Min Lee [a*], Dong-Seong Sohn [b], Young-Soo Han [a]
[a]*Korea Atomic Energy Research Institute, 989-111 Daedeok-daero, Yuseong-gu, Daejeon 34057, Republic of Korea*
[b]*Ulsan National Institute of Science and Technology, 50 UNIST-gil, Eonyang-eup, Uljoo-gun, Ulsan 689-798, Republic of Korea*
[*]*Corresponding author: cmlee@kaeri.re.kr*

1. Introduction

Zirconium alloys have been utilized as fuel cladding tube since 1960s due to their adequate mechanical strength, acceptable corrosion resistance, and low thermal neutron absorption cross-section. However, many researchers reported that zirconium alloys have some disadvantages during an accident such as loss of coolant accident (LOCA). During a LOCA, cladding temperature can increase to approximately 1200 ºC, at which the oxidation rate becomes relatively high, so that the claddings can be easily failed. After the Fukushima accident, more concerns have arisen over the accident resistance of zirconium alloy cladding tube. To overcome this issue, accident tolerant fuels (ATF) are widely researched in these days.

To develop fuel cladding tubes with improved accident resistance, it is also important to understand the basic oxidation behaviors of zirconium alloys at high-temperature. Hence, here, we conducted high-temperature steam oxidation tests using Zr-1Nb-1Sn-0.1Fe cladding tube at 800-1200 ºC. After the tests, microstructures of the specimens were elaborately analyzed using optical microscopy (OM), scanning electron microscopy (SEM), and transmission electron microscopy (TEM). Morphology of zirconium alloys, propagation of cracks in the oxides, and precipitates were analyzed in detail, and the results will be presented.

2. Methods and Results

Experiments were performed using Zr-1Nb-1Sn-0.1Fe cladding tube specimens. The length, outer diameter, and thickness of each specimen were 40, 9.5, and 0.57 mm, respectively. After the specimens were prepared, they were oxidized in a radiant heating furnace shown in Fig. 1 [1–7]. The specimen was located between two alumina specimen holders to avoid reaction with the Inconel holder. The condition within the furnace was maintained as steam by making steam flow to the furnace 15 min before starting a test; the steam flow rate was maintained as 3.5 mg/(cm^2·s) throughout the test.

After the tests, the specimens were analyzed using OM, SEM, TEM, and EPMA. For this analysis, a small ring was cut from a specimen, and it was mounted on the hot mount resin, ground using silicon carbide papers (320, 600, and 800 grit), and polished using diamond suspensions (6, 3, and 1 mm). OM and SEM were used to observe the overall microstructures. OM images were

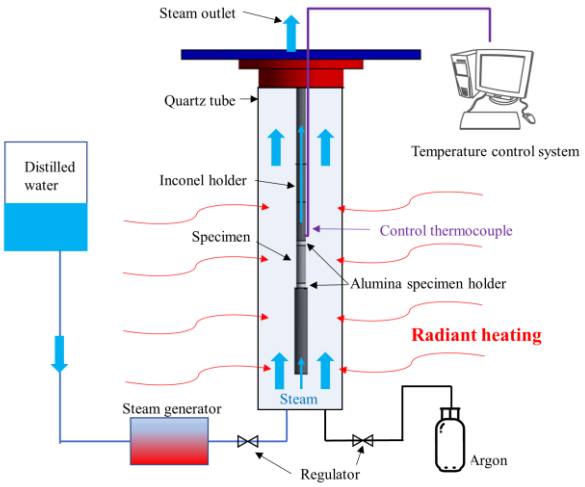

Fig. 1. Schematic of the radiant heating furnace used for the high-temperature steam oxidation tests.

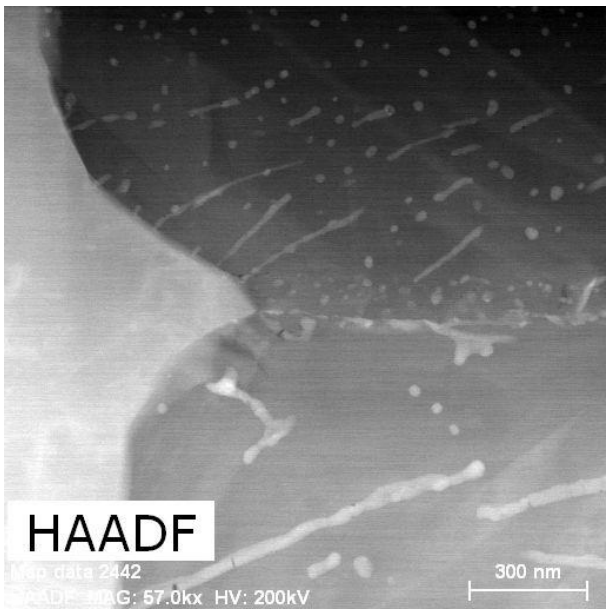

Fig. 2. High angle annular dark field scanning transmission electron microscopy image of the oxide-metal interface after oxidation at 1000 ºC.

taken using the DMI3000B, and SEM images were taken using the Quanta 200FEG in the backscattered electron (BSE) mode at 15 kV. TEM was used to analyze the precipitates within the oxide layer. The TEM specimens were prepared using the focused ion beam (FIB) milling method, and the Helios NanoLab 450 microscope was used. The TEM specimens were analyzed using the JEM-2100F.

3. Conclusions

Fig. 2 shows a high angle annular dark field (HAADF) scanning transmission electron microscopy (STEM) image of the oxide-metal interface after the oxidation at 1000 ºC. The zirconium substrate is shown at the left side of the figure, and the oxide is shown at the right side of the figure. In the oxide, many white particles can be observed. They are precipitates, and they are brighter than the oxides due to their high atomic mass. It was concluded that most of them are Zr-Sn intermetallic or β-Nb.

REFERENCES

[1] C. M. Lee, Y. -K. Mok, and D. -S. Sohn, High-Temperature Steam Oxidation and Oxide Crack Effects of Zr-1Nb-1Sn-0.1Fe Fuel Cladding, Journal of Nuclear Materials, Vol.496, p.343, 2017.
[2] C. M. Lee, H. Y. Jeong, A. Yoon, Y. -K. Mok, and D. -S. Sohn, Microstructural Analysis of Preformed Oxides on a Zirconium Alloy before and after Subsequent Oxidation at 1000–1200 °C, Corrosion Science, Vol.139, p.410, 2018.
[3] C. M. Lee, and D. -S. Sohn, Enhanced High-Temperature Oxidation Resistance of a Zirconium Alloy Cladding by High-Temperature Preformed Oxide on the cladding, Corrosion Science, Vol.131, p.116, 2018.
[4] C. M. Lee, H. Y. Jeong, A. Yoon, Y. -K. Mok, and D. -S. Sohn, Microstructural Characteristics and Different Effects of 800-1200 ºC Preformed Oxides on High-Temperature Steam Oxidation of a Zirconium Alloy Cladding, Journal of Alloys and Compounds, Vol.753, p.119, 2018.
[5] C. M. Lee, H. -J. Lee, H. -G. Kim, Y. -K. Mok, Y. -S. Han, and D. -S. Sohn, Effect of Pre-Oxidation Temperature on the Ductility of a Zirconium Alloy Cladding under Simulated Accident Conditions, Journal of Nuclear Materials, Vol.515, p.80, 2019.
[6] C. M. Lee, Y. -S. Han, Y. -K. Mok, and D. S. Sohn, Study of Mechanism of Oxidation Resistance Enhancement Induced by Preformed Oxide on Zirconium Alloys, Corrosion Science, Vol.158, p.108105, 2019.
[7] C. M. Lee, G. Kim, D. -S. Sohn, Y. -S. Han, and Y. -K. Mok, Short Communication on “Self-Crack-Healing Behavior of Oxide Formed on a Zirconium Alloy Cladding Tube”, Journal of Nuclear Materials, Vol.526, p.151749, 2019.